

# Supplementary Information

## Theoretically Informed Entangled Polymer Simulations: Linear and Non-Linear Rheology of Melts

Abelardo Ramírez-Hernández,<sup>a</sup> Marcus Müller,<sup>b</sup> and Juan J. de Pablo<sup>\*a</sup>

### 1 Algorithm for the slip-link creation process

In this section we describe the algorithm adopted to create new SL pairs. As explained in the main text, the dynamics of the links and chains are such that it is possible for one ring to leave its chain, *i.e.*  $s_k \notin [0, N-1]$ ; when this occurs, this ring and its corresponding partner are destroyed, and a new SL pair is created as follows:

- Select a chain-end at random, and place the first SL on that chain-end with position  $\mathbf{R}_k(s_k)$ .
- Create a list of all  $m$  segments (a “segment” consists of two successive or bonded beads along the chain) within a distance  $r_{cut}$  from the first SL. The cutoff distances  $r_{cut}$  is chosen to be larger than  $b_{sl}$ .
- Select a random position  $\mathbf{R}_{n_k}(s_{n_k})$  (where  $n_k$  is the partner of the  $k$ th SL) along a randomly chosen segment with probability  $p = \exp[-\beta u_{sl} \{ \mathbf{R}_k(s_k) - \mathbf{R}_{n_k}(s_{n_k}) \}] / C_{norm}$ . The normalization constant  $C_{norm}$  is given by  $C_{norm} = \sum_{l=1}^m C_l$ , where  $C_l$  is the contribution of the  $l$ th segment, explicitly:

$$C_l = \int_0^1 \exp[-\beta u_{sl} \{ \mathbf{R}_k(s_k) - (\mathbf{r}_i + s_{n_k} \Delta \mathbf{r}) \}] ds_{n_k} \\ = \sqrt{\frac{\pi}{6}} \frac{b_{sl}}{|\Delta \mathbf{r}|} \exp \left[ -\frac{3}{2b_{sl}^2} (\mathbf{r}_i - \mathbf{R}_k)^2 + \frac{3}{2b_{sl}^2} \frac{|\Delta \mathbf{r} \cdot (\mathbf{r}_i - \mathbf{R}_k)|^2}{|\Delta \mathbf{r}|^2} \right] \times \\ \left\{ \operatorname{erf} \left[ \sqrt{\frac{3}{2b_{sl}^2}} \left( |\Delta \mathbf{r}| + \frac{\Delta \mathbf{r} \cdot (\mathbf{r}_i - \mathbf{R}_k)}{|\Delta \mathbf{r}|} \right) \right] - \operatorname{erf} \left[ \sqrt{\frac{3}{2b_{sl}^2}} \frac{\Delta \mathbf{r} \cdot (\mathbf{r}_i - \mathbf{R}_k)}{|\Delta \mathbf{r}|} \right] \right\} \quad (1)$$

where  $\Delta \mathbf{r} = \mathbf{r}_{i+1} - \mathbf{r}_i$ ,  $|\Delta \mathbf{r}|$  is the magnitude and  $\operatorname{erf}(x)$  is the error function. Note that a SL pair is only replaced at a chain-end if its length is smaller than  $r_{cut}$ .

### 2 Distribution of slip-Links along chain backbone

Figure S1 shows the distribution of entanglements along the chain. For this calculation, we use chains of  $N = 128$  beads and  $N_{sl}^o = 32$  slip-links per chain ( $k = 1.5625, \chi = 0$ ). As can be seen in the figure, the distribution is uniform.

<sup>a</sup> Department of Chemical and Biological Engineering, University of Wisconsin-Madison, Madison, Wisconsin 53706, E-mail: depablo@engr.wisc.edu

<sup>b</sup> Institut für Theoretische Physik, Georg-August-Universität, 37077 Göttingen, Germany.

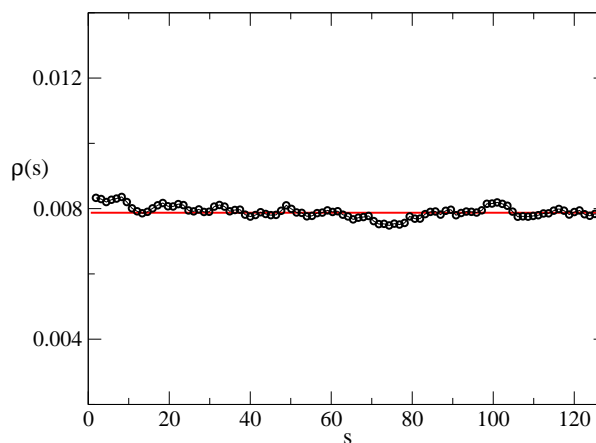


**Figure S 1** Distribution of sliplinks along the chains' contour for  $N = 128$  and  $N_{sl}^o = 32$ .

### 3 Computing loss and storage modulus

To compare our simulations with experimental data we first compute the stress relaxation function,  $G(t)$ , defined by  $G(t) = G_0 \langle \Sigma_{\alpha\beta}(t) \Sigma_{\alpha\beta}(0) \rangle$ , where  $\alpha$  and  $\beta$  are two orthogonal axes,  $G_0 = k_B T n N / V$ . The stress,  $\Sigma_{\alpha\beta}(t)$ , which contains only contributions arising from intramolecular interactions, is given by

$$\sigma_{\alpha\beta}(t) = \frac{3k_B T}{V} \sum_{i=1}^n \sum_{s=1}^{N-1} \frac{b_{i\alpha}(s,t) b_{i\beta}(s,t)}{b^2} \\ = \frac{k_B T}{V} \sqrt{nN} \Sigma_{\alpha\beta}(t), \quad (2)$$

where  $b_{i\alpha}(s,t)$  is the  $\alpha$ -component of the bond vector ( $\mathbf{b}_i(s) = \mathbf{r}_i(s+1) - \mathbf{r}_i(s)$ ) that connects the  $s$  and  $s+1$  beads on the  $i^{\text{th}}$  chain. The time correlation functions required to calculate  $G(t)$  are computed using a version of the order- $n$  algorithm<sup>1,2</sup>. The rationale behind our choice of only consider intramolecular interaction in the stress calculation is as follows: intermolecular interactions do not differ between a simple monomeric liquid and the corresponding polymeric melt and, therefore, their relative contribution to the stress decreases as the macromolecules increase their length and the elastic stress contribution dominates<sup>3,4</sup>. Note that for short

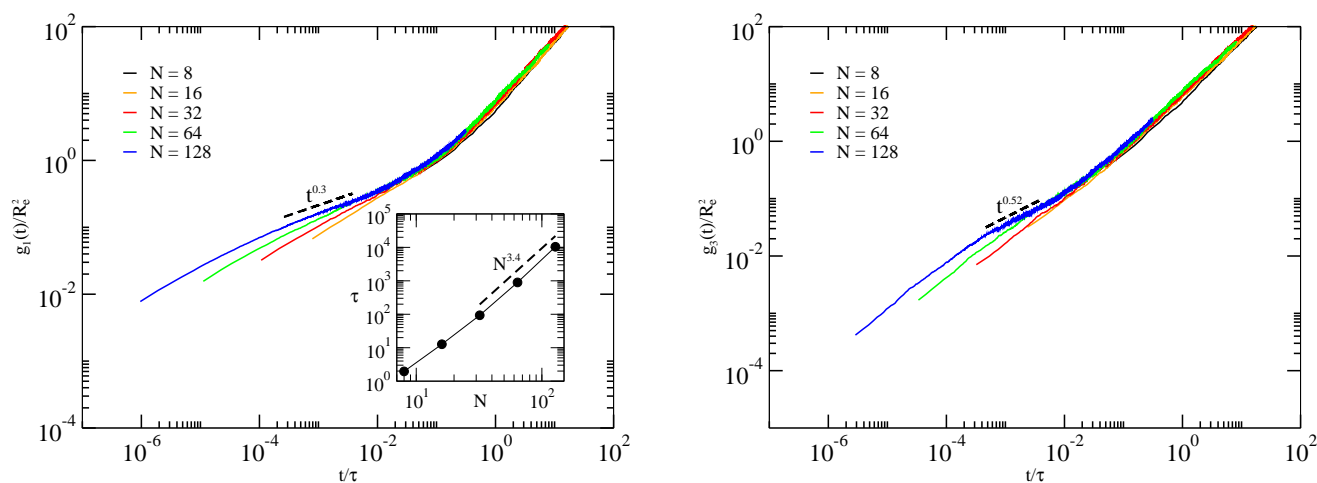


**Figure S 2** Temporal evolution of the mean square displacements for: (left) beads  $g_1(t)$  and (right) center of mass of the chains,  $g_3(t)$ , for different polymerization index  $N = 8, 16, 32, 64, 128$ , as indicated. In  $g_1(t)$ , a regime with a  $t^{0.3}$  scaling can be seen at intermediate times where  $g_3(t)$  grows as  $t^{0.52}$ . Inset: The longest relaxation time  $\tau = R_c^2/D$ , as a function of  $N$ , where  $D$  is obtained by the long-time behavior of  $g_3(t)$ . The dashed line is a power law fit with exponent 3.4.

chains this could not be true and the intermolecular stress contribution should be taken into account. On the other hand, Likhtman *et al.*<sup>5</sup> have found that for a single-chain slip-spring model, a contribution of the slip-spring should be taken into account in the stress calculation. The entanglements are an emergent property from the intermolecular interactions, and due our argument above regarding those contributions, here we adopt the view that the main contribution to the stress is only that related to the intramolecular interaction.

From the stress relaxation function, we extract the loss and storage modulus,  $G'$  and  $G''$ , by fitting  $G(t)$  to a sum of Maxwell modes:  $G(t) = G_0 \sum_p a_p \exp[-t/\tau_p]$ . Once the parameters  $a_p$  and  $\tau_p$  are obtained we use the following expressions:

$$\frac{G'(\omega)}{G_0} = \sum_p \frac{a_p (\omega \tau_p)^2}{1 + (\omega \tau_p)^2}, \quad (3)$$

and

$$\frac{G''(\omega)}{G_0} = \sum_p \frac{a_p \omega \tau_p}{1 + (\omega \tau_p)^2}. \quad (4)$$

#### 4 Scaling laws for the mean square displacements

In this section we show that the model proposed here displays the scaling laws expected from tube models. To do that, we have performed simulations for different polymerization indexes,  $N = 8, 16, 32, 64, 128$  (representing an increasing molecular weight by fixing the average bond length to a reference value), and we have computed the mean-squared displacement for beads and for the chain center-of-mass. For ho-

mopolymers we use again  $\chi = 0$ , and parameter  $\kappa$  is fixed at  $\kappa = 1.5625$ . Figure S2 shows results for the mean-squared displacements,  $g_1(t)$  and  $g_3(t)$ , as a function of time. It can be seen that, at short times, the bead displacements,  $g_1(t)$ , exhibit a scaling behavior with a power law  $t^{0.5}$ ; at intermediate times,  $g_1(t)$  enters a regime with a power law  $t^{0.3}$  as the molecular weight increases; eventually we observe a crossover to regular diffusion at long times. The mean-squared displacement for the center-of-mass,  $g_3(t)$ , also exhibits sub-diffusive behavior at intermediate times, with a scaling law  $t^{0.52}$ , very close to the  $t^{1/2}$  predicted by the tube model; at long times, regular diffusion is attained. From the long time behavior of  $g_3(t)$ , we compute the longest relaxation time,  $\tau$ , as a function of molecular weight. As expected,  $\tau$  is a monotonically increasing function of  $N$ ; for large  $N$ , the longest relaxation time grows approximately as  $N^{3.4}$ ; as  $N$  increases, we observe a crossover from a weaker  $N$ -dependence to the  $N^{3.4}$  law (see inset of Figure S2).

#### 5 Scaling laws for viscosity

Figure S3 shows results for the steady shear viscosity,  $\eta = \sigma_{xy}/\dot{\gamma}$ , as a function of shear rate for homopolymers of different molecular weight. The results are shown in dimensionless units. We performed simulations for several polymerization indexes,  $N = 32, 64, 128$ , and explored the response of melts to different applied shear rates,  $\dot{\gamma}$ . As we increase the molecular weight, the shear thinning regime appears at higher shear rates, consistent with experiments. In the shear-thinning regime, the viscosity follows a power law scaling as  $\eta \sim \dot{\gamma}^\mu$ , with  $\mu = -0.78$ . This exponent is in good agreement with that

found experimentally<sup>6,7</sup>.

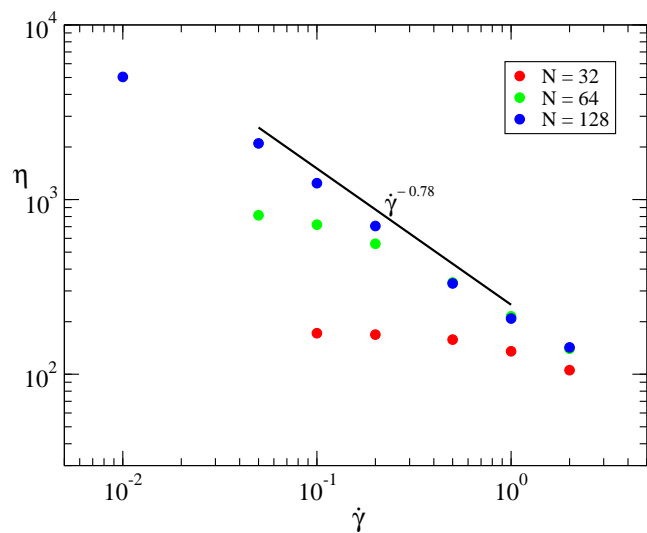


**Figure S 3** Steady shear viscosity as a function of the shear rate, for different polymerization index  $N$ .

## References

- 1 D. Frenkel and B. Smit, *Understanding Molecular Simulations* Academic Press, Second Edition 2002.
- 2 D. Dubbeldam, D. C. Ford, D. E. Ellis and R. Q. Snurr, *Molec. Simulation* **35**, 1084 (2009).
- 3 M. Doi and S. F. Edwards, *The Theory of Polymer Dynamics* Oxford, 1986.
- 4 M. Müller and K. Ch. Daoulas, *J. Chem. Phys.* **129**, 164906 (2008).
- 5 J. Ramírez, S. K. Sukumaran and A. E. Likhtman, *J. Chem. Phys.* **126**, 244904 (2007).
- 6 R. A. Stratton, *J. Colloid Interf. Sci.* **22**, 517 (1966).
- 7 D. Nichetti and I. Manas-Zloczower, *J. Rheol.* **42**, 951 (1998).